Influence of columnar defects on vortex dynamics in $Bi_2Sr_2CaCu_2O_8$ from out-of-plane and flux transformer transport measurements

W. S. Seow, R. A. Doyle, and A. M. Campbell
IRC in Superconductivity, University of Cambridge, CB3 0HE, England

G. Balakrishnan and D. McK. Paul
Department of Physics, University of Warwick, Coventry, CV4 7AL, England

K. Kadowaki
National Research Institute for Metals, 1-2-1, Sengen, Tsukuba-Shi, Ibaraki 305, Japan

G. Wirth
Gesellschaft für Shwerionenforschung, Planckstr 1, D-64291, Darmstadt, Germany

The c-axis resistivity, $\rho_c(B,T,\theta)$, where θ is the angle between the c axis and the dc field, has been measured for $Bi_2Sr_2CaCu_2O_8$ single crystals before and after the introduction of columnar defects by heavy ion irradiation. The effects of different columnar track density and angle with respect to the basal plane are also investigated. Uniaxial enhancement of the irreversibility line for fields below the matching field and parallel to the columnar defects is observed in out-of-plane transport measurements. Measurements in the flux transformer geometry confirm that the vortices are connected lines in the irradiated crystal. We have also attempted to reconcile c-axis data with the predictions of the Bose-glass theory for correlated disorder. [S0163-1829(96)01621-9]

INTRODUCTION

Layered high-temperature superconductors (HTS) are anisotropic, and $Bi_2Sr_2CaCu_2O_8$ (BSCCO) in particular, has a resistive anisotropy, ρ_c/ρ_{ab}, of 10^5. When a magnetic field is applied along the c axis, this material is expected to form two-dimensional (2D) Abrikosov pancake vortices in the superconducting layers, coupled by Josephson strings in the interlayers, instead of the usual vortex lines formed in 3D superconductors. Because of the weak Josephson coupling between the planes, only small energies are required to decouple the 2D pancake vortices in adjacent layers from each other. This means that the vortex ''lines'' are extremely sensitive to thermal fluctuations. In the case of weak random disorder (the usual as-produced state for these systems) individual pancakes, which are not themselves strongly pinned, may easily be driven off pins since there is little restoring force from pancakes more strongly pinned in adjacent layers due to the small tilt modulus, C_{44}. This process results in flux cutting and dissipation, and has the effect of lowering the temperature dependent irreversibility field below which the superconductor is technologically useful to well below B_{c2}.

In as produced BSCCO crystals Busch *et al.*[1] have shown convincing evidence using transport measurements in the flux transformer geometry that vortices always have a longitudinal correlation (cutting) length much smaller than typical crystal thicknesses. Thus the vortices can be regarded as a set of independent pancakes rather than a continuous line with finite line tension over macroscopic distances. Further evidence for the quasi-2D nature of BSCCO in the mixed state is related to observations that dissipation is determined only by the component of the field parallel to the c axis and is independent of the current direction.[2–6]

On the other hand, there is much experimental evidence[7–12] to support the fact that pancake vortices pinned by columnar tracks in heavy-ion irradiated BSCCO crystals behave as well-coupled vortex lines at fields up to the matching field, B_Φ. The pinning is strongest when the magnetic field is aligned or close to alignment with the columnar tracks. Klein *et al.*[8] first reported evidence suggesting that vortices in BSCCO crystals, irradiated with heavy ions at 45° from the c axis, display signatures indicating that the vortices behave as well correlated lines. The magnetization of these crystals at temperatures above 50 K showed uniaxial enhancement of the magnetization curves when the magnetic field was applied parallel to the columnar tracks. In contrast to point disorder which promotes vortex line wandering and entanglement, correlated disorder caused by heavy ion irradiation (HII) inhibits wandering and promotes localization of the vortex lines. This implies that the low lying irreversibility line in highly anisotropic materials is not intrinsically limited by the low dimensionality, but may also be considerably altered by careful engineering of the disorder. It also raises the question of the relative contributions of Lorentz-force driven and other sources of dissipation (related to the low dimensionality) in as-produced and irradiation damaged materials, a central issue addressed in this paper. In particular, the HII is expected to change the electromagnetic or Josephson coupling between the copper oxide bilayers (dimensionality), and enhance the apparent tilt modulus, C_{44}, in the mixed state[13] of BSCCO.

The framework of the Bose-glass theory developed by Nelson and Vinokur[14,15] has become a common technique to study the effects of correlated disorder in HTS crystals and

films. By accounting for vortex pinning and creep,[10,12] the theory is able to predict current-voltage characteristics,[16] the existence of a transition temperature into the Bose-glass phase,[8,10,16–20] and the frequency dependence of the vortex dynamics.[12,21] Its predictions have been shown to have extensive validity in YBa$_2$Cu$_3$O$_{7-\delta}$,[18–22] and have also been used to extract various parameters in BSCCO (Refs. 7, 9–12, 16) and Tl$_2$Ba$_2$CaCu$_2$O$_8$ thin films.[17] However, as recently pointed out by Zech *et al.*,[7] the complex shape of the irreversibility line in BSCCO after heavy ion irradiation cannot be derived by Bose-glass theory, indicating that it may need extension in the very anisotropic systems. Further, there are no explicit predictions, nor have there been any experimental investigations, of the Bose glass in the *c*-axis behavior of HTS crystals.[23,24] Thus an investigation of possible Bose-glass–like features in the out of plane behavior of BSCCO is attempted in this work.

All of the existing work on heavy ion irradiated BSCCO crystals including both general phenomenological,[7,8,25–27] as well as Bose-glass analyses,[7,10–12,16] have been carried out using magnetic measurements. This is at least partly due to the difficulty of obtaining low resistance contacts, and achieving reasonable electric field sensitivity in the linear regime, without incurring the considerable local heating which is known to occur in BSCCO crystals,[28] even using moderate currents. Transport measurements have been carried out on thin films of BSCCO (Ref. 9) and Tl$_2$Ba$_2$CaCu$_2$O$_8$ (Ref. 17) but it remains important to perform transport measurements on single crystals which contain far less random quenched disorder when compared with thin film systems. This is a further important motivation for this study.

Determination of the out-of-plane behavior of single crystals of the very anisotropic HTS systems is well known to be a powerful means of investigating the normal state electronic behavior,[29] and also the properties in the mixed state.[4] When both the magnetic field and transport current are applied parallel to each other, the Lorentz force disappears and one obtains a force free configuration. Then rotation of one of either the field or current (usually the magnetic field) allows a direct investigation of the effects of Lorentz force driven contributions to dissipation. There has been considerable speculation about the dissipation processes in HTS crystals, due to the apparent lack of Lorentz force dependence mentioned above. Various models including fluctuation effects,[4,30–32] flux cutting and curved flux lines,[33] series stack of Josephson tunnel junctions,[5] and thermally activated phase slippage[34] are some of the models proposed to explain this apparent lack of Lorentz force dependence. These have either only been shown to fit moderately anisotropic materials like La$_{2-x}$Sr$_x$CuO$_4$ and YBa$_2$Cu$_3$O$_{7-\delta}$, or have had limited ranges of applicability. On the other hand, there is also some evidence to suggest that thermally activated flux flow (TAFF) induced dissipation also occurs in BSCCO films[2,9,35] and crystals,[36,37] even in the Lorentz force-free configuration. Moreover the possible effects of columnar disorder on this apparent Lorentz force-free dissipation have never been systematically investigated despite being an obvious critical test for such models. The force-free configuration is generally attractive in its own right since a finite $J\|B$ tends to produce helical instabilities in vortex arrays[6] and in entangled flux

liquids. This instability leads to a linear resistivity, just as for currents perpendicular to the vortex lines. Brandt[38] has shown that a nonzero shear modulus in a weakly pinned Abrikosov lattice resists this instability, suggesting that $J\|B$ is an excellent geometry in which to study vortex dynamics.[39]

In this paper, we report on *c*-axis and flux transformer geometry transport measurements on as-produced and heavy-ion irradiated Bi$_2$Sr$_2$CaCu$_2$O$_8$ (BSCCO) crystals with different doses and directions of irradiation. Extracted irreversibility temperatures, $T_{irr}(B,\theta)$, show that there is indeed locking in of vortex lines with large accommodation angles, θ_a, after irradiation. Anisotropic enhancement of $T_{irr}(B,\theta)$, when the applied magnetic field is aligned (or nearly aligned) to the columnar tracks is observed. The flux transformer geometry measurements show that the pancake vortices show linelike features only after irradiation when the applied field is parallel to the columnar tracks. Investigation of the form of the resistivity curves approaching the superconducting state in addition to $T_{irr}(B,\theta)$ has been carried out. We find, in agreement with many studies, that the dissipation in pristine samples is not determined simply by the Lorentz force. The conditions of applied field angle which result in Arrhenius-like behavior for the resistivity are explored. Before irradiation, Arrhenius-like behavior is found for all angles except when the field is very close to alignment with the *ab* planes. After irradiation Arrhenius-like behavior is observed for all angles and fields except for the case where the field is below the matching field and parallel to the defects. Then a power-law-like behavior is apparent, reminiscent of the various glass models for HTS. In the absence of any detailed theory we naively apply the predictions of Bose-glass theory directly to the out-of-plane behavior of irradiated crystals. The qualitative features are in surprising agreement with expectations. Thus we are able to extract the combined critical exponents $[n=v'(z'-2)]$ (Ref. 15) and the Bose-glass transition temperature, $T_{BG}(B,\theta)$, from our resistivity data. Remarkably, these values agree reasonably well with previously published data[9,17] and appear to consolidate the validity of the Bose-glass predictions even when applied to out-of-plane data for BSCCO.

EXPERIMENTAL DETAILS

Boules of BSCCO were grown separately by two different groups using the travelling floating-zone technique in double-ellipsoidal infrared furnaces. Optically smooth rectangular crystals from the two different batches were cleaved and cut from larger mosaics. Batch 1 (crystals K1 and K2) has a transition temperature, T_c, determined using the inflection point of the resistive transition of the crystals in the remnant field of our magnet (about 5 mT), of 87 K while batch 2 (crystals W1, W2, and W3) has a T_c value of 89 K. The crystal dimensions were all close to 0.25 mm in width and 0.8 mm in length except for crystal K2 which was close to 0.25×0.30 mm^2. The thicknesses of the crystals are all between 15–20 μm. Four 25 μm gold wires were attached to both the top and bottom faces of the crystals using Du Pont 6838 silver epoxy and were then mounted onto a quartz substrate. They were then annealed at 475 °C for 5 min in flowing O$_2$ to attach the contacts. The resulting contact resistance

(of a pair of contacts including lead resistance) is typically less than 4 ohms. The out-of-plane room temperature resistivity was $\rho_c = 1.6$ Ω cm. A measurement current of 100 μA (approx. 0.05 A/cm^2) was used for samples W1, W2, W3, and K1, and 10 μA (approx. 0.013 A/cm^2) for crystal K2, at a frequency of 77 Hz to maximize the sensitivity of our measurements without encountering heating or inducing nonlinear effects. These current densities allow a 4 to 5 order drop in magnitude (relative to the normal state value at 120 K) in resistance below T_c to be measured. Comparison of voltages from pairs at different distances from the current injection electrodes shows close agreement and confirms that the current density is satisfactorily uniform (due to the large anisotropy) when injected along the c axis. This is true for all fields and temperatures. All measurements were made at fields greater than or equal to 0.1 T. Thus they are unaffected by the well known and pronounced effects of surface[40] and geometrical barriers[41] which affect the irreversible behavior of these anisotropic systems in the transverse geometry in fields of order of the lower critical field, H_{c1}.

Crystals W1, W2, and K1 were irradiated at GSI Darmstadt, with 2.25 GeV Au ions. A matching field, B_Φ, is defined where the vortex spacing, $a_0 \approx (\Phi_0/B)^{1/2}$, equals the average defect spacing determined by the radiation dose. Crystals W1 and W2 were irradiated to a matching field, B_Φ, of 0.5 T and crystal K1 with $B_\Phi = 2$ T. Crystals W2 and K1 were irradiated with the beam directed perpendicular to the ab planes of the crystals while crystal W1 was irradiated with the beam 45° off the c axis of the crystal. Crystals K2 and W3 were measured in the as-produced state. Given that the threshold energy for creating columnar tracks is 16 keV/nm in BSCCO,[42] it is certain that columnar tracks are produced along the entire thickness of the crystal, since the crystals are not more than 20 μm thick. After irradiation, the normal state c-axis resistances were increased by approximately 15% while the T_c values were reduced by approximately 2.5 K for the 0.5 T matching field and 3 K for the 2 T matching field doses, respectively. The crystals were mounted on a cryogenic goniometer assembly that allowed the crystals to be rotated with respect to the applied field with a resolution of ~0.1°. Alignment of the crystals is made with respect to the minimum in resistivity when the applied field is aligned parallel to the ab planes. The columnar tracks are estimated to be within 2–3° of the intended angles with respect to the basal planes since the crystals are mechanically stabilized on the substrates only by the measurement leads which prevents careful alignment with respect to the substrates without incurring damage in the crystal. Since several crystals are irradiated at once, it is very difficult to align each one better than aligning all of the substrates.

RESULTS AND DISCUSSION

A. Irreversibility line

We begin with a discussion of the angular dependence of the irreversibility line (IL), which is defined here as a line of constant c-axis resistivity, ρ_c, close to where this vanishes below our sensitivity. This behavior, for both cases of before (BI) and after irradiation (AI) with the case of columnar defects introduced parallel to the c axis, are compared and discussed. The irreversibility temperature, $T_{\mathrm{irr}}(B,\theta)$, for a

given applied field, is defined where the c-axis resistivity reaches a criterion of 1×10^{-4} Ω. Recently, there has been much debate about the physical significance of the IL defined using various criteria, in different regimes of field and temperature in BSCCO crystals. Majer, Zeldov, and Konczykowski[43] have explicitly shown that the magnetic hysteresis and hence the onset of magnetic reversibility, in low fields and at temperatures above about 76 K, is entirely caused by geometrical barriers. However, at applied fields much larger than the penetration field, the temperature where the c-axis resistivity vanishes approaching the superconducting state has been shown to correspond closely to the temperature where the c-axis critical current density obtained from IV measurements becomes finite.[44] Although a finite criterion has to be imposed on the determination of the IL, the temperature and field dependencies of the resistivity components are anyway important in their own right. The IL in irradiated samples can moreover be correlated with disorder induced pinning over a wider range of fields and temperatures than for pristine crystals, since it is shifted well beyond the penetration field even at high temperatures approaching T_c. As pointed out by Radzihovsky,[45] the IL in irradiated crystals can be interpreted as the locus where the vortex lattice freezes into a superconducting Bose glass of vortices localized on columnar defects and this is determined by the matching field rather than the fields associated with vortex penetration at high temperatures.

Figure 1(a) shows the $B - T_{\mathrm{irr}}(B,\theta)$ phase diagram for several angles, θ, for a pristine sample (crystal K2). We define θ as the angle between the applied field and the c axis so that $\theta = 0$ corresponds to $B \| c$. The irreversibility lines are shown for angles of $\theta = 0°, 45°, 60°, 75°,$ and 90° only for the sake of clarity. The IL moves toward higher temperatures as we rotate the field away from the c axis. In the force-free configuration [the lowest curve in Fig. 1(a)] the field is applied parallel to the current and the c axis of the crystal. As the field is rotated away from the c axis [moving toward higher curves in Fig. 1(a)] one would expect that, in an isotropic material, the increasing Lorentz force would act increasingly strongly on the vortices. Then the resistance of the sample should increase as expected if the dissipation is determined by thermally activated flux flow (TAFF) under the action of an increasing Lorentz force as the field is rotated away from the c axis of the crystal. This is contrary to what is observed and suggests that the relevant parameters for dissipation are not the relative angle between the current and field (Lorentz force) but only the field direction with respect to the crystallographic axes. What is less clear is whether this discrepancy arises simply from the intrinsic anisotropy of the material or from a non-Lorentz force determined (fluctuation related) dissipation mechanism. It is important in this respect to note that the IL for the as-produced crystal, at different θ, are very similar in form. Blatter, Geshkenbein, and Larkin (BGL) (Ref. 46) have derived simple general scaling functions for the IL for isotropic uncorrelated disorder in very anisotropic HTS materials. That work predicts that $B_{\mathrm{irr}}(T,\theta) = B_{\mathrm{irr}}(T, \theta = 0°)/\varepsilon(\theta)$ where $\varepsilon^2 = \cos^2\theta + 1/\gamma^2 \sin^2\theta$ and $\gamma^2 = m_c^*/m_{ab}^*$ is the effective mass anisotropy. For large anisotropy and for angles not too close to the ab planes, this collapses to $B_{\mathrm{irr}}(T,\theta) = B_{\mathrm{irr}}(T, \theta = 0°)/\cos(\theta)$. Zech et al.[7] have recently claimed experimental verification of these pre-
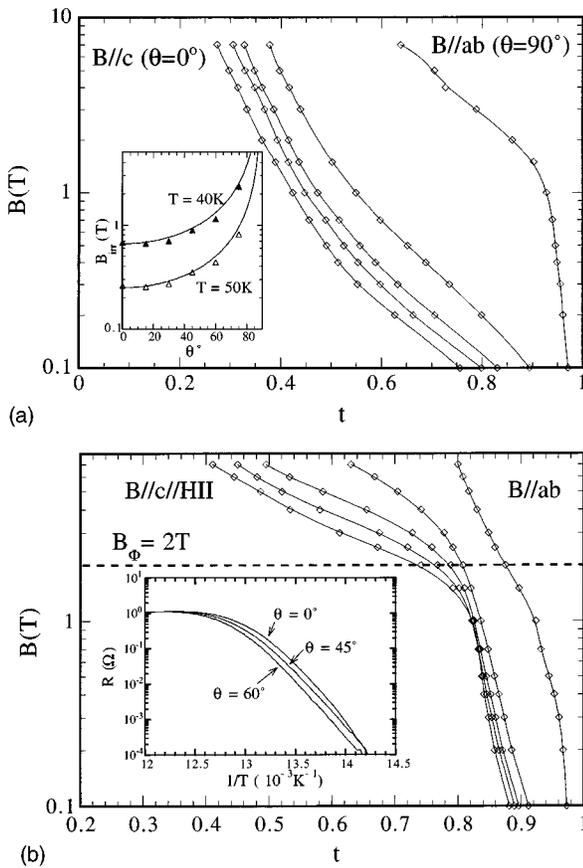
FIG. 1. (a) The field dependence of the resistively determined irreversibility temperature, $T_{irr}(B,\theta)$, for the pristine crystal (crystal K2) at various angles (0°, 45°, 60°, 75°, and 90°) of applied field relative to the c axis. 0° corresponds to $B \| c$ axis and $t = T_{irr}/T_c$. Lines are guides for the eye. The inset shows the angular dependence of $B_{irr}(T,\theta)$ at $T = 40$ and 50 K for crystal K2. Solid lines are fits to the function $B_{irr}(T, \theta=0°)/\cos(\theta)$. (b) As for (a) but for the irradiated crystal K1 ($B_\Phi=2T$). $B \| c \|$ HII indicates that the applied magnetic field is parallel to the c axis of the crystal and the heavy ion irradiation columnar defects. Lines are guides for eye. The inset shows Arrhenius plots for the same crystal for $\theta=0°$, 45°, and 60° at $B=0.5$ T.

FIG. 2. The irreversibility temperature, $T_{irr}(B,\theta)$, plotted as a function of θ, where θ_a is the accommodation angle, for crystal W2 ($B_\Phi=0.5$ T, irradiation parallel to c axis). Lines are guides for the eye.

dictions for all angles except when B is very close to the ab planes (within about 5°) using magnetization data on similar BSCCO crystals to those studied here. They show good scaling for all fields and temperatures for applied field angles up to 45° from alignment with the c axis. A similar construction to theirs is shown in the inset to Fig. 1(a) where the angular behavior without irradiation at 40 and 50 K as well as the fit to the BLG prediction above is presented. There is satisfactory agreement up to at least 45° from the c axis. In the measurements here the Lorentz force increases sinusoidally as the field is rotated away from the c axis (and the current). Nevertheless this result is in good agreement with vector magnetization data on similar crystals and a detailed discussion will be presented in Ref. 47.

Figure 1(b) shows the IL of an irradiated crystal (crystal K1), with $B_\Phi=2$ T where the irradiation and damage is parallel to the c axis. After irradiation by heavy ions, the IL's are clearly and strongly enhanced for all fields measured here and this is most pronounced below the matching field. There

are four main results: (i) that the IL's lie almost on top of each other over a wide range of "accommodation" angles, defined as the angular range over which the irreversibility line is angle independent due to vortices being "locked" onto the columnar defects, for $\theta<45°$; (ii) the IL again develops clear angular dependence for $B \geq B_\Phi$; (iii) for $B \gg B_\Phi$ the IL converges toward that of the pristine sample as also shown in Refs. 7,26; and (iv) that the IL after irradiation and for fields below the matching field assume a slope, $\Delta B_{IL}/\Delta T$ very similar to the case for $B\|ab$ of the pristine sample.

The behavior of crystal (W2) which was irradiated with a smaller dose corresponding to $B_\Phi=0.5$ T is qualitatively identical. However the accommodation angle, θ_a, appears slightly larger than for crystal K1, with $\theta_a\approx60-75°$. This is apparent from the data in Fig. 2, where we have plotted $T_{irr}(B,\theta)$ as a function of θ for four different fields. For $B<B_\Phi$, $T_{irr}(B,\theta)$ remains almost unaffected when the field is rotated away from alignment with the defects. This holds until approximately 60° (indicated by the arrow) where $T_{irr}(B,\theta)$ starts to increase. Close inspection of the data in Fig. 1(b) indicates that an estimation for θ_a of 60° at $B=1.0$ T is not unreasonable. The data at 75° or for $B\|ab$ is however considerably shifted relative to smaller angles below the matching field. On the other hand, above the matching field where $B>B_\Phi$, $T_{irr}(B,\theta)$ regains a pronounced angular dependence. The values for θ_a which are determined here are consistent with those obtained by van der Beek *et al.*[11] using transmittivity techniques on BSCCO single crystals as well as those measured in Ref. 17 from the angular dependence of the resistivity of $Tl_2Ba_2CaCu_2O_8$ thin films. These values also compare favorably with that of $\theta_a=30°$ obtained for $YBa_2Cu_3O_{7-\delta}$ single crystals.[19] The important point is not so much the precise values variously obtained for the accommodation angle but that these are consistently very large. This is an artifact of the large anisotropy of the material. θ_a can be recalculated taking into account this large anisotropy, thereby yielding a corrected value which would be measured if the crystal was to be "stretched" along its c direction by a factor of the resistivity anisotropy. This isotropic-equivalent geometrical correction yields a "squeezed" angle of 0.4° for crystal W2 and 0.2° for crystal K1. These are
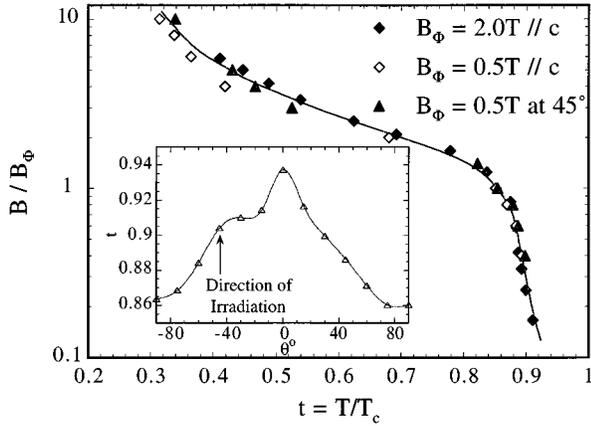
FIG. 3. Scaled irreversibility temperatures as a function of reduced field, B/B_Φ, for all three irradiated crystals. Crystals W2 and K1 are irradiated parallel to the c axis with doses equivalent to $B_\Phi = 0.5$ and 2 T, respectively. Crystal W1 is irradiated at an angle of 45° to the c axis to a matching field, $B_\Phi = 0.5$ T. The inset shows the uniaxial enhancement, for an applied field of 0.4 T, of $T_{\text{irr}}(B, \theta)$ for crystal W1. Again, the lines are guides for the eye.

slightly smaller than the "squeezed" angle for YBa$_2$Cu$_3$O$_{7-\delta}$ of 4.3°.[19] The inset in Fig. 1(b) shows the resistive curves for crystal K1 in an Arrhenius plot for $B = 0.5$ T and $\theta = 0°$, 45°, and 60°. It clearly indicates that, despite the fact that the $T_{\text{irr}}(B, \theta)$ values are very close for $0 < \theta < 45°$, the flux flow state shows significantly different curvature at different angles. The data only becomes Arrhenius-like (linear on this construction) for angles larger than the estimated accommodation angle of 60°. This is discussed in more detail below.

Above the matching field, for $B > B_\Phi$, the behavior becomes more complicated as there are now more vortices than the number of columnar tracks and therefore the "extra" vortices sit on interstitial sites between the columnar tracks.[45] It is important to determine the extent to which vortex-vortex interactions with vortices which are pinned on the columns determines the behavior of interstitial vortices. Vortices pinned on the columns are immobile, but in addition have considerably enhanced apparent tilt modulus. This may affect both the shear and tilt responses of interstitial vortices subjected to both Lorentz forces and thermal fluctuations. The shape of the IL after irradiation bears a significant resemblance to the IL when B is applied parallel to the ab planes for the as-produced crystal. This is not surprising since the ab planes may themselves be regarded as a kind of correlated disorder, due to the strong modulation of the order parameter along the c axis. In both cases of intrinsic pinning by the planes, and pinning by columnar defects, lock-in or accommodation angles can be defined, and the mechanism for dissipation is likely to be nucleation and growth of kinks in the pinned vortices off the linear defects, rather than activation off pointlike defects which dominates when there is a finite angle between the field and the linear defect.

Figure 3 shows that the IL for three irradiated crystals can be scaled on top of each other, despite different doses and directions of irradiation. This shows the universality of our conclusions for each crystal. Further, it implies that the vortex interaction with the columnar defects is not sensitive to

the direction of the columns with respect to the basal plane (at least for the angles studied here). This is also strong evidence that the columnar defects control the dissipation and pinning to fields well above B_Φ. However, as shown by the data here and that from other sources,[7,26] at fields much larger than B_Φ, the IL eventually converges to the IL of the pristine samples when the vortex spacing becomes much smaller than the column spacing so that vortex-vortex interactions begin to dominate over the correlated disorder.

B. Uniaxial enhancement of the IL and flux transformer measurements

The inset of Fig. 3 shows the anisotropic enhancement of $T_{\text{irr}}(B, \theta)$ as a function of θ for crystal W1 ($B_\Phi = 0.5$ T at 45° to c axis) at $B = 0.4$ T. It occurs, as expected, when B is aligned with the columnar tracks. It supports conclusions from magnetic measurements[7,8,10–12] suggesting that vortices in heavy ion irradiated crystals of BSCCO are well coupled rather than consisting of independent pancakes when B is applied parallel to the correlated disorder. The peak of the enhancement in $T_{\text{irr}}(B, \theta)$ does not appear to correspond exactly to the direction of irradiation. This may be understood by consideration of the decreasing $T_{\text{irr}}(B, \theta)$ with increasing θ. Superposition of the decreasing $T_{\text{irr}}(B, \theta)$ with the enhancement of $T_{\text{irr}}(B, \theta = 45°)$ (direction of irradiation) leads to the peak of the enhancement being slightly shifted to lower θ, rather than occurring exactly at $\theta = 45°$. It is also possible that there could be some contribution to this shift from a slight misalignment (2–3°) of the crystal with respect to the direction of irradiation. In either case the directional enhancement is clear and must arise from the columnar defects.

In order to further elucidate the linelike nature of the vortices, measurements using the flux transformer geometry have been made on the same crystal. This geometry is a sensitive test of the longitudinal correlation of moving vortices. It involves injecting current into one of the large (ab) faces of the crystal, while simultaneously but separately measuring the voltage drop across that face (top voltage) and the opposite face (bottom voltage). For magnetic fields with a component normal to ab plane, these voltages are determined by the velocity of vortices crossing the electrodes. The large anisotropy of the crystals means that the current distribution is highly nonuniform, so vortices only feel a significant Lorentz force at the side of the crystal where the current is injected. If the vortices have a large line tension (correlation length larger than the crystal thickness) then they maintain their coherence through the thickness of the crystal and have identical velocities along their lengths despite the nonuniform force. On the other hand, if the vortices have a small or vanishing tilt modulus (correlation length smaller than the crystal thickness), then flux cutting and rearrangement takes place through the thickness of the crystal so that the bottom voltage is smaller than the top voltage. Measurement of the temperature dependence of the voltages allows one to investigate how this correlation length changes and whether it ever matches the crystal thickness. In pristine BSCCO, reported data[1] indicates that this longitudinal correlation length is much smaller than typical crystal thicknesses for all temperatures but there are, to our knowledge, no existing studies of heavy ion irradiated crystals using this tech-
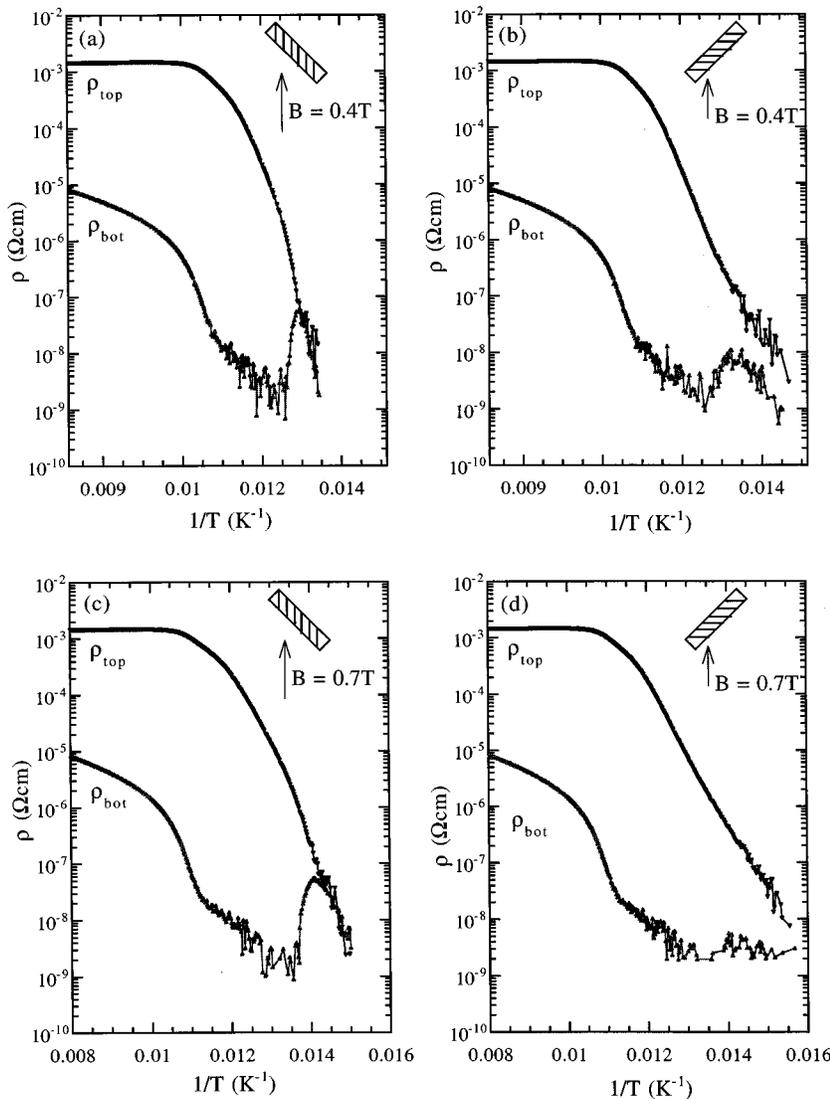
FIG. 4. Top (primary) and bottom (secondary) apparent resistivities (voltage/current density) of the flux transformer geometry data for crystal W1. (a) and (c) show the behavior of the irradiated crystal at fields of 0.4 and 0.7 T applied parallel to the columnar defects while (b) and (d) show identical data for the case of the field applied normal to the columns. These configurations are shown schematically in the insets to the figures.

nique. Figure 4 thus presents, from flux transformer measurements, the effect of heavy ion irradiation damage on the longitudinal correlation of vortices in BSCCO. For clarity, the figure shows the "apparent resistivities" rather than the voltages. These "resistivities" are calculated from the measured top and bottom voltages when current is injected in the top face, assuming uniform current distribution across the thickness of the crystal. ρ_{top} is the "resistivity" calculated using the top voltage pair while ρ_{bot} is the "resistivity" from the bottom voltage pair. The real resistivities, which take into account the highly nonuniform current distribution which results from the large anisotropy, were also calculated from the top and bottom voltages using Busch's modified Montgomery analysis.[1,48] The calculated c-axis resistivities yield good agreement with the c-axis resistivities measured directly.

Crystal W1 is most instructive for this investigation since it was irradiated at 45° to the c axis to a matching field of 0.5 T. This allows direct comparison of the behavior when B is parallel and antiparallel to the defects, but always at the same angle with respect to the basal planes. In Figs. 4(a) and 4(c), B is aligned parallel to the columnar defects whereas Figs. 4(b) and 4(d) show the results when the field is applied 90° away from the columnar tracks. These configurations are il-

lustrated schematically in the figures. It is clear that the bottom voltages in Figs. 4(a) and 4(c) converge to the same value as the top voltages before disappearing below our experimental sensitivity while this does not occur when the field is antiparallel to the defects in Figs. 4(b) and 4(d). Since matched voltages mean that the flux line velocity at the top and bottom faces are the same, this strongly suggests well correlated vortex line motion which implies that vortices in BSCCO display "linelike" features after heavy ion irradiation, as previously observed by magnetic measurements.[8] The "hump" in the bottom voltage appears in a rather narrow temperature window (about 5 K) before this voltage merges with the top voltage just prior to both disappearing below the available sensitivity. This may be explained by a temperature dependent increase in the correlation length of the vortices at temperatures just above the second order phase transition from an entangled vortex liquid into the Bose-glass phase. Figure 4(b) also shows a small maximum in the bottom or secondary resistivity close to where this vanishes. Such a peak was also observed by Busch *et al.*[1] The c-axis resistivity, $\rho_c(T)$, increases through a peak while the in-plane resistivity, $\rho_{ab}(T)$, decreases monotonically and therefore the anisotropy, $\rho_c(T)/\rho_{ab}(T)$ goes through a maxi-

mum. This causes a minimum in the effective penetration depth of the current, and hence a minimum in the bottom voltage at slightly higher temperatures than the hump. It cannot however cause the two voltages to become equal unless the vortices are well correlated and the c-axis resistivity vanishes. In $YBa_2Cu_3O_{7-\delta}$, which is considerably less anisotropic ($\gamma \approx 6$ rather than about 250 in BSCCO) it has been shown elsewhere[49–52] that the primary and secondary voltages in the flux transformer geometry become equal well above the irreversibility temperature. Recently, however, Lopez *et al.*[53] have shown that this only occurs in twinned samples. In twin free $YBa_2Cu_3O_{7-\delta}$ crystals, the voltages meet at the same temperature where they disappear discontinuously at a supposed first order melting transition. Thus the observation of matched vortex velocities at the top and bottom faces of anisotropic crystals when current is injected on the top face appears to be universally associated with the presence of correlated disorder. This is an important observation. Further theoretical work is needed to explain exactly how the correlated disorder is able to have such a remarkable effect in the flux flow state where the vortices sense the disorder dynamically.

C. Resistivity

Figure 5(a) shows an Arrhenius plot of the resistivity of crystal W1 both for the case when B is applied parallel to, as well as 90° away from, the columnar tracks (which lie at 45° to the ab planes). It is clearly seen that for B parallel to the columnar tracks, the behavior is nonlinear, but for the case where B is not aligned with the columnar tracks, the resistivity is indeed linear and thus Arrhenius-like below about 1% of the normal state resistivity. This is also the case for crystals W2 and K1, i.e., dose and damage angle independent. We note, however, that the behavior returns to a linear Arrhenius-like dependence on $1/T$ for $B > B_\Phi$ in all cases. In comparison, Arrhenius plots for the unirradiated crystals show linearity for all angles except for B parallel to the planes (within 2–3°). The curvature in the Arrhenius plots (which is only present when the magnetic field is applied parallel to the columnar defects) is consistent with Bose-glass theory [which predicts a power law behavior, $\rho \sim (T - T_{BG})^{v'(z'-2)}$] for in-plane resistivity and this is discussed below. Finally, it is noted that the c-axis activation energies $U(T=0$ K, $B)$ extracted from the pristine crystals with B applied parallel to the c axis give a similar field dependence [$U(0,B) \sim B^{-0.25}$] (Ref. 37) and magnitude (50–80 meV) to previous reports[36] so that we expect that our conclusions are general. After irradiation, the apparent activation energies are increased by about an order of magnitude (regardless of θ). This results from the increased pinning in the irradiated samples. It must however be emphasized that the curvature in the Arrhenius plots when the field is applied parallel to the columnar tracks makes the usual linear fit to extract U very difficult and criterion dependent. Nevertheless, it is not unreasonable to expect a large enhancement of the activation energy, U, given the striking upward shift of the resistively determined irreversibility line. Gerhauser *et al.*[25] obtained a much smaller enhancement of about a factor of 2 from magnetic relaxation measurements at 10 K and ascribed this to the small tilt modulus in BSCCO. This observation is not
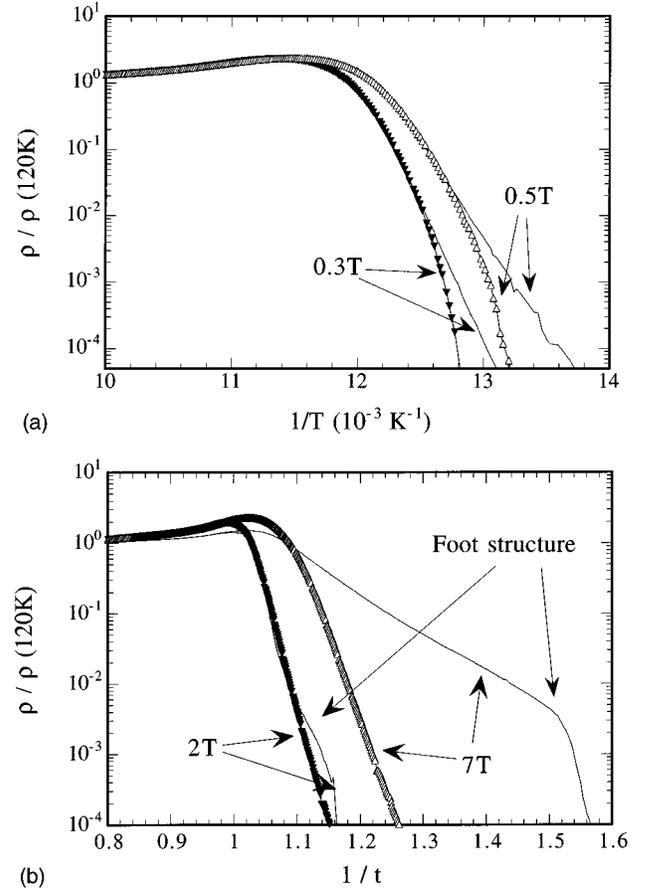
FIG. 5. (a) Arrhenius plot showing the behavior of the c-axis resistivity when magnetic fields of 0.3 and 0.5 T are applied at $\theta=45°$ (parallel to the columnar tracks) and $\theta=-45°$ (perpendicular to columnar tracks) for crystal W1 ($B_\Phi=0.5$ T irradiated at 45° from c axis). Symbols are used for the data for $\theta=45°$, while the data for $\theta=-45°$ is shown by the thin lines. (b) Arrhenius plot for irradiated crystal K1 (symbols) and pristine crystal K2 (thin lines) at $\theta=90°$ (parallel to the ab planes) at $B=2$ and 7 T. The foot structure is clearly indicated in the figure and is discussed in the text.

inconsistent with the data in this paper. Their values are measured at low temperatures and well below the irreversibility line, a regime we cannot access from transport measurements. Further, the irreversibility field is already very large at 10 K so that it may not be surprising that only small enhancements in U may be achieved by increased disorder at this temperature. Miu *et al.*[9] have also recently reported only a small enhancement (at $t=T/T_c=0.9$) in U in BSCCO thin films after heavy ion irradiation. Our data is equally well reconciled with theirs taking into account the increased enhancement in U which they predict for lower temperatures.

Another interesting and related question concerns the out-of-plane transport behavior of the very anisotropic layered HTS materials when the magnetic field is applied parallel to the ab planes. This is the obvious configuration for investigation of Josephson (Fraunhofer) behavior if the c axis is really Josephson coupled in the superconducting state in BSCCO since the field is then applied parallel to the layers while the current is injected across them. Although the crystals in this study are in the (extreme) large junction limit,

being much larger than the *c* axis or Josephson penetration depth, it is still instructive to investigate this geometry. Figure 5(b) shows the Arrhenius representation of the resistivity when *B* is applied parallel to the *ab* planes both for a pristine (crystal K2) and an irradiated crystal (crystal K1). The foot-like structure, indicated by the arrow in the figure, has been observed before and is always observed in sufficiently high quality crystals. Lock-in transitions of vortices aligned with the superconducting planes (intrinsic pinning) or correlated disorder have been discussed in detail by Blatter *et al.*,[23] Zavaritsky,[54] on the other hand, has suggested that this sudden drop in resistivity might be due to a dimensional (2D to 3D) transition of the vortices. In the configuration in Ref. 54 and in Fig. 5(b), *J* is parallel to the *c* axis and *B* is almost aligned with the planes. This is the maximum Lorentz force configuration but should not sense intrinsic pinning since the force is directed parallel rather than normal to the layers.[55] Consequently the vortices are driven along the planes between the interlayers. There is no large restoring force (pinning) acting against this at high temperatures and this explains the long activated tail. At lower temperatures, the resistance vanishes rapidly at the irreversibility temperature. One possibility is that thermal fluctuations are sufficiently reduced so that the average displacement of any vortex segment becomes smaller than the layer spacing and the vortices finally lock-in between the planes. Another is that there is a field induced transition in the Josephson coupling of the *c* axis. There has been rather little attention paid to this geometry, mostly due to the difficulty of aligning crystals sufficiently accurately with the field. More work is thus required to resolve this issue. However, careful checks indicate that the columnar defects in the irradiated samples suppress or damp this rapid transition and hence the sudden drop in resistivity is not observed. The thermally activated tail is still present above this due to the maximum Lorentz force though. Finite pinning of vortex pancakes with moments normal to the planes cannot however be precluded and these will always prevent very accurate alignment of the internal field with the *ab* planes in such measurements.

D. Bose-glass analysis

Finally, the applicability of the Bose-glass theory to the *c*-axis data presented above is considered. Within the framework of the Bose-glass model, the (in-plane) resistivity $\rho(T)$ should vanish as the temperature T approaches the Bose-glass transition temperature, $T_{BG}(B,\theta)$, from above as $\rho(T) \sim (T - T_{BG})^{v'(z'-2)}$.[15] Thus a plot of $\rho(T)/(d\rho/dT)$ against T should give a linear plot.[56,57] Because of the apparent absence of Lorentz force dependence, and the similar absence of explicit predictions for behavior in the Bose-glass phase for *c*-axis transport, we have attempted to apply the theory for the in-plane resistivity directly and without correction to the *c*-axis resistivity. This will be seen to be reasonably justified in what follows. It is now also clear that the first order transitions close to the IL in $YBa_2Cu_3O_{7-\delta}$ (Ref. 53) and BSCCO (Ref. 58) intimately associate loss of coherence in the in- and out-of-plane directions. Figure 6 presents a plot of $\rho(T)/(d\rho/dT)$ and $\rho(T)$ on separate axes as a function of T for crystal K1 at $B = 0.7$ T parallel to the *c* axis of the crystal. Reasonably linear behavior below $T = 75$ K is
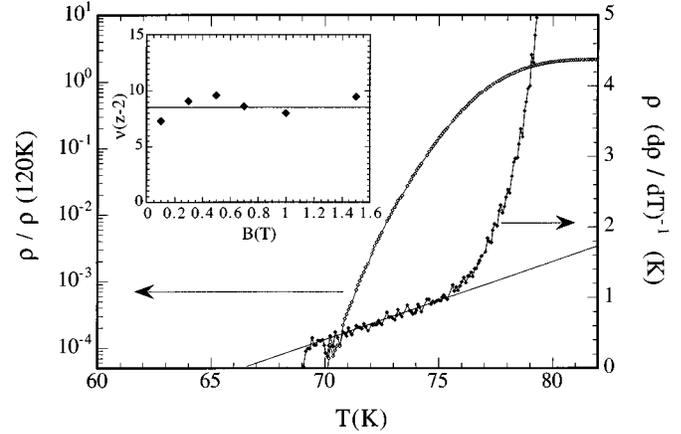
FIG. 6. Plot of $\rho(d\rho/dT)^{-1}$ and $\rho/\rho(120\ \mathrm{K})$ versus temperature for 0.7 T applied parallel to the *c* axis and the columnar defects for crystal K1, where ρ is the *c*-axis resistivity. The linear regime of $\rho(d\rho/dT)^{-1}$ is clearly seen below 75 K and is shown by the extrapolated line. The inset shows the Bose-glass exponent $n = v'(z'-2)$ extracted from the resistivity data.

apparent suggesting the onset of a regime where the glass prediction holds. It is important to note that this is precisely the regime where Arrhenius-like behavior was observed before irradiation. We found that a free three parameter fit to the resistive tail in order to evaluate glassy behavior in pristine and irradiated samples is extremely unsatisfactory. The field dependence of the values for the exponent, $n[= v'(z'-2)]$, are plotted in the inset of Fig. 6. The average value is $n \approx 8.5$. Figure 7 shows the field dependence of $T_{BG}(B,\theta=0°)$ extracted from the linear regime plot of $\rho(T)/(d\rho/dT)$ against T and the $T_{irr}(B,\theta=0°)$ extracted with a finite criterion for crystal K1. These are compared to the IL of the same crystal before irradiation. There is remarkable similarity between this plot of $T_{BG}(B,\theta=0°)$ and that ex-
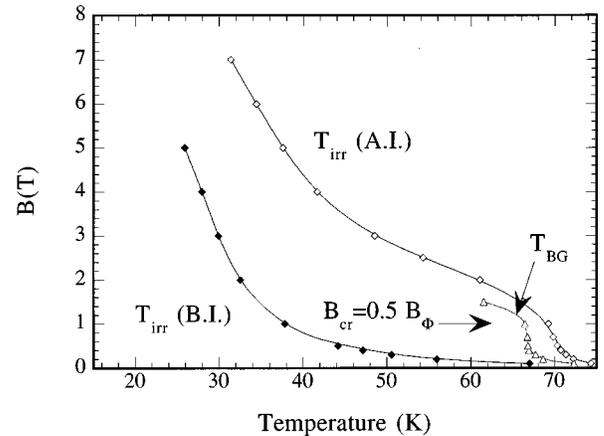
FIG. 7. Resistively determined IL for crystal K1 before (closed diamonds) and after irradiation (open diamonds). Also shown are the Bose-glass temperatures (open triangles) extracted using the construction in Fig. 6. The magnetic fields are applied parallel to the *c* axis of the crystal. $T_{BG}(B,\theta=0°)$ is only presented for $B < B_\Phi$ for reasons discussed in the text. Lines are guides for the eye.

tracted by Zech *et al.*[7] who measured the in-plane behavior from their magnetization data. There is a clear crossover field at about $0.5B_\Phi$ as observed elsewhere in both $YBa_2Cu_3O_{7-\delta}$ (Ref. 20) and BSCCO (Refs. 7,9,16) and this has been quite extensively discussed in Ref. 20.

We return briefly to the value for the exponent. It must be emphasized that there is considerable scatter in reported values for the glass exponent, both for vortex and Bose-glass phases. Budhani, Holstein, and Suenaga[17] obtained n values of $(3.6–4.5)\pm0.3$ for $Tl_2Ba_2CaCu_2O_8$ thin films irradiated at $B_\Phi = 3.1$ T, whereas Miu *et al.*[9] reported an average n value of 9, for $B < B_\Phi$ at $B_\Phi = 1$ T from in-plane transport measurements of BSCCO thin films. On the other hand, Gammel, Schneemeyer, and Bishop[56] determined a vortex glass exponent $v(z-1) = 6.5 \pm 1.5$ for $YBa_2Cu_3O_{7-\delta}$ single crystals, while Safar *et al.*[57] have reported $v(z-1) \approx 7 \pm 1$ for BSCCO crystals (from in-plane transport data). Simulations using a simplified model of lattice bosons[59] yield estimates of 3.5–4.5 for the n value. Clearly, the vortex glass and Bose-glass phases are not easily distinguishable using these exponents. Nelson and Vinokur have suggested that the best way to distinguish the two phases are by use of data obtained by tilting the magnetic field away from the c axis. In the experimental geometry here, increasingly Arrhenius-like behavior is found when the magnetic field is tilted away from the c axis below B_Φ or indeed for $B \geq B_\Phi$ for any alignment. This results in a quadratic dependence of the dependent variable, $\rho/(d\rho/dT)$, on T in the construction of Fig. 6 so that a linear fit to the tail to extract the $T_{BG}(B,\theta)$ or critical exponent becomes very sensitive to the chosen range of T for the fit. This means, strictly speaking, that Bose-glass parameters can only clearly be identified when the field is below the matching field and applied very close to alignment with the defects, even though this may correspond to the force free configuration. The rapid disappearance of this behavior for small tilting angles of the field is in good agreement with expected helical instability in this configuration, but in apparent contradiction with the large accommodation angles presented in Fig. 2 and discussed above. What this means is that the temperature dependence of the resistivity is a more sensitive probe of vortex behavior than $T_{irr}(B,\theta)$ itself. We are unable to say whether the Bose glass phase is suppressed by Lorentz force or whether it really exists in a large range of accommodation angles but that evaluation thereof is masked by the details of our measurement. This is an interesting question for future experiments.

Nevertheless, the angular dependence may be evaluated by mapping the angular dependence of $T_{irr}(B,\theta)$ for pristine and irradiated crystals. Figure 8 presents experimental data in the form suggested by Nelson and Vinokur[15] for discriminating between vortex- and Bose-glass behavior. It requires fixing the field component parallel to the c axis while increasing the in-plane component of the field and simultaneously measuring the glass temperature. Here the irreversibility temperatures, $T_{irr}(B,\theta)$, are used rather than the glass temperatures both for pristine and irradiated crystals. Figure 8 shows this construction for crystal W2 where the field component parallel to the c axis is fixed at 0.5 T. There is a remarkable resemblance of our plot to the predicted cusplike shape by Nelson and Vinokur.[15] The irreversibility temperature, $T_{irr}(B,\theta)$, for the unirradiated crystal (W3), on the other
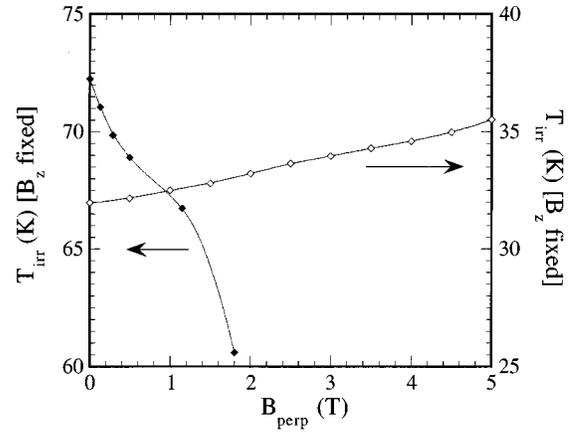
FIG. 8. Angular dependence of $T_{irr}(B,\theta)$ of the irradiated crystal W2 and the unirradiated crystal W3 for fixed B_z parallel to the c axis when the field component parallel to the ab planes, B_{perp}, is increased. (Closed diamonds: crystal W2, $B_z = 0.5$ T; open diamonds: crystal W3, $B_z = 1.5$ T.) Lines are guides for the eye.

hand, shows the upward parabolic curvature expected from a vortex-glass phase. It is difficult to say that this is strong support for the existence of either vortex- or Bose-glass phases, since the critical parameters are unable to be extracted except for the Bose glass for $B \| c$ and $B < B_\Phi$. Nevertheless the remarkable similarity between the construction in Fig. 8 and that in Ref. 15, in addition to the agreement between the measured $T_{BG}(B,\theta = 0°)$ in Fig. 7 and those obtained in Ref. 7 for in-plane behavior, should be useful for development of theoretical predictions for the behavior of the out-of-plane transport behavior.

CONCLUSIONS

In conclusion, significant enhancement in the irreversibility lines of heavy ion irradiated $Bi_2Sr_2CaCu_2O_8$ crystals is shown from c-axis transport measurements, and even in the force free geometry. Uniaxial enhancement of the IL for fields below the matching field and parallel to the columnar tracks is observed from transport measurements on this system. Flux transformer geometry measurements confirm the linelike behavior of the vortices in the irradiated crystals when the applied field is aligned to the columnar tracks. The resistivities become non-Arrhenius-like for fields below the matching field applied parallel to the columnar tracks. The data show several signatures predicted by Bose-glass theory when we apply this to the c-axis resistivity. This should assist in extension of such theories to explain the c-axis behavior of very anisotropic HTS systems.

ACKNOWLEDGMENTS

[1] R. Busch, G. Ries, H. Werthner, G. Kreiselmeyer, and G. Saemann-Ischenko, Phys. Rev. Lett. **69**, 522 (1992).

[2] P. H. Kes, J. Aarts, V. M. Vinokur, and C. J. van der Beek, Phys. Rev. Lett. **64**, 1063 (1990).

[3] D. H. Kim, K. E. Gray, R. T. Kampwirth, and D. M. McKay, Phys. Rev. B **42**, 6249 (1990).

[4] K. Kadowaki, Y. Songliu, and K. Kitazawa, Supercond. Sci. Technol. **7**, 519 (1994) and references therein.

[5] K. E. Gray and D. H. Kim, Phys. Rev. Lett. **70**, 1693 (1993).

[6] Z. Hao, C.-R. Hu, and C. S. Ting, Phys. Rev. B **51**, 9387 (1995).

[7] D. Zech, S. L. Lee, H. Keller, G. Blatter, B. Janossy, P. H. Kes, T. W. Li, and A. A. Menovsky, Phys. Rev. B **52**, 6913 (1995).

[8] L. Klein, E. R. Yacoby, Y. Yeshurun, M. Konczykowski, and K. Kishio, Phys. Rev. B **48**, 3523 (1993).

[9] L. Miu, P. Wagner, A. Hadish, F. Hillmer, H. Adrian, J. Wiesner, and G. Wirth, Phys. Rev. B **51**, 3953 (1995).

[10] M. Konczykowski, N. Chikumoto, V. M. Vinokur, and M. V. Feigelman, Phys. Rev. B **51**, 3957 (1995).

[11] C. J. van der Beek, M. Konczykowski, V. M. Vinokur, T. W. Li, P. H. Kes, and G. W. Crabtree, Phys. Rev. Lett. **74**, 1214 (1995).

[12] C. J. van der Beek, M. Konczykowski, V. M. Vinokur, G. W. Crabtree, T. W. Li, and P. H. Kes, Phys. Rev. B **51**, 15 492 (1995).

[13] A. E. Koshelev, P. Le Doussal, and V. M. Vinokur (unpublished).

[14] D. R. Nelson and V. M. Vinokur, Phys. Rev. Lett. **68**, 2398 (1992).

[15] D. R. Nelson and V. M. Vinokur, Phys. Rev. B **48**, 13 060 (1993).

[16] V. V. Moshchalkov, V. V. Metlushko, G. Güntherodt, I. N. Goncharov, A. Yu Didyk, and Y. Bruynseraede, Phys. Rev. B **50**, 639 (1994).

[17] R. C. Budhani, W. L. Holstein, and M. Suenaga, Phys. Rev. Lett. **72**, 566 (1994).

[18] W. Jiang, N.-C. Yeh, D. S. Reed, U. Kriplani, D. A. Beam, M. Konczykowski, T. A. Tombrello, and F. Holtzberg, Phys. Rev. Lett. **72**, 550 (1994).

[19] N.-C. Yeh, D. S. Reed, W. Jiang, U. Kriplani, M. Konczykowski, and F. Holtzberg, Physica C **235-240**, 2659 (1994).

[20] L. Krusin-Elbaum, L. Civale, G. Blatter, A. D. Marwick, F. Holtzberg, and C. Field, Phys. Rev. Lett. **72**, 1914 (1994).

[21] D. S. Reed, N.-C. Yeh, M. Konczykowski, A. V. Samoilov, and F. Holtzberg, Phys. Rev. B **51**, 16 448 (1995).

[22] G. W. Crabtree, J. Fendrich, W. K. Kwok, and B. G. Glagola, Physica C **235-240**, 2643 (1994).

[23] G. Blatter, M. V. Feigel'man, V. B. Geshkenbein, A. I. Larkin, and V. M. Vinokur, Rev. Mod. Phys. **66**, 1125 (1994).

[24] A. E. Koshelev (private communication).

[25] W. Gerhäuser, G. Ries, H. W. Neumüller, W. Schmidt, O. Eibl, G. Saemann-Ischenko, and S. Klaumünzer, Phys. Rev. Lett. **68**, 879 (1992).

[26] J. R. Thompson, Y. R. Sun, H. R. Kerchner, D. K. Christen, B. C. Sales, B. C. Chakoumakos, A. D. Marwick, L. Civale, and J. O. Thomson, Appl. Phys. Lett. **60**, 2306 (1992).

[27] A. Ruyter, V. Hardy, Ch. Goupil, J. Provost, D. Groult, and Ch. Simon, Physica C **235-240**, 2663 (1994).

[28] R. A. Doyle (private communication).

[29] N. E. Hussey, J. R. Cooper, J. M. Wheatley, I. R. Fisher, A. Carrington, A. P. Mackenzie, C. T. Lin, and O. Milat, Phys. Rev. Lett. **76**, 122 (1996).

[30] S. Sarti, R. Fastampa, M. Giura, E. Silva, and R. Marcon, Phys. Rev. B **52**, 3734 (1995).

[31] R. Ikeda, T. Ohmi, and T. Tsuneto, J. Phys. Soc. Jpn. **60**, 1051 (1991).

[32] R. Ikeda, T. Ohmi, and T. Tsuneto, Phys. Rev. Lett. **67**, 3874 (1991).

[33] A. M. Campbell and J. E. Evetts, Adv. Phys. **21**, 199 (1972).

[34] G. Briceno, M. F. Crommie, and A. Zettl, Phys. Rev. Lett. **66**, 2164 (1991).

[35] P. Wagner, F. Hillmer, U. Frey, and H. Adrian, Phys. Rev. B **49**, 13 184 (1994).

[36] K.-H. Yoo, D. H. Ha, Y.-K. Park, and J. C. Park, Phys. Rev. B **49**, 4399 (1994).

[37] J. H. Cho, M. P. Maley, S. Fleshler, A. Lacerda, and L. N. Bulaevskii, Phys. Rev. B **50**, 6493 (1994).

[38] E. H. Brandt, J. Low Temp. Phys. **44**, 33 (1981); **44**, 59 (1981).

[39] D. Kumar, M. G. Blamire, R. A. Doyle, A. M. Campbell, and J. E. Evetts, J. Appl. Phys. **76**, 2361 (1994).

[40] M. Konczykowski, F. Rullier-Albenque, E. R. Yacoby, A. Shaulov, Y. Yeshurun, and P. Lejay, Phys. Rev. B **43**, 13 707 (1991).

[41] E. Zeldov, A. I. Larkin, V. B. Geshkenbein, M. Konczykowski, D. Majer, B. Kyaykovich, V. M. Vinokur, and H. Shtrikman, Phys. Rev. Lett. **73**, 1428 (1994).

[42] M. Leghissa, Th. Schuster, W. Gerhäuser, S. Klaumünzer, M. R. Koblischka, H. Kronmüller, H. Kuhn, H.-W. Neumüller, and G. Saemann-Ischenko, Europhys. Lett. **19**, 323 (1992).

[43] D. Majer, E. Zeldov, and M. Konczykowski, Phys. Rev. Lett. **75**, 1166 (1995).

[44] S. Lou, G. Yang, and C. E. Gough, Phys. Rev. B **51**, 6655 (1995).

[45] L. Radzihovsky, Phys. Rev. Lett. **74**, 4923 (1995).

[46] G. Blatter, V. B. Geshkenbein, and A. I. Larkin, Phys. Rev. Lett. **68**, 875 (1992).

[47] R. A. Doyle, W. S. Seow, L. F. Cohen and J. Totty (unpublished).

[48] H. C. Montogomery, J. Appl. Phys. **42**, 2971 (1971).

[49] D. López, G. Nieva, and F. de la Cruz, Physica C **235-240**, 2575 (1994).

[50] H. Safar, P. L. Gammel, D. A. Huse, S. N. Majumdar, L. F. Schneemeyer, D. J. Bishop, D. López, G. Nieva, and F. de la Cruz, Phys. Rev. Lett. **72**, 1272 (1994); Physica C **235-240**, 2581 (1994).

[51] Yu. Eltsev, W. Holm, and Ö. Rapp, Phys. Rev. B **49**, 12 333 (1994).

[52] F. de la Cruz, D. López, and G. Nieva, Philos. Mag. B **70**, 773 (1994).

[53] D. López, E. F. Righi, G. Nieva, and F. de la Cruz (unpublished).

[54] V. N. Zavaritsky, Physica C **235-240**, 2715 (1994).

[55] R. A. Doyle, A. M. Campbell, and R. E. Somekh, Phys. Rev. Lett. **71**, 4241 (1993).

[56] P. L. Gammel, L. F. Schneemeyer, and D. J. Bishop, Phys. Rev. Lett. **66**, 953 (1991).

[57] H. Safar, P. L. Gammel, D. J. Bishop, D. B. Mitzi, and A. Kapitulnik, Phys. Rev. Lett. **68**, 2672 (1992).

[58] R. A. Doyle, D. Liney, W. S. Seow, A. M. Campbell, and K. Kadowaki, Phys. Rev. Lett. **75**, 4520 (1995).

[59] M. Wallin and S. M. Girvin, Phys. Rev. B **47**, 14 642 (1993).